ELSEVIER

Journal of Alloys and Compounds 408–412 (2006) 1145–1148

Journal of ALLOYS AND COMPOUNDS

www.elsevier.com/locate/jallcom

Lattice constants and electron gap energies of nano- and subnano-sized cerium oxides from the experiments and first-principles calculations

S. Tsunekawa [a,*], J.-T. Wang [b], Y. Kawazoe [a]

[a] *Institute for Materials Research, Tohoku University, Sendai 980-8577, Japan*
[b] *Institute of Physics, Chinese Academy of Sciences, Beijing 100080, China*

Received 30 July 2004; received in revised form 26 October 2004; accepted 15 December 2004
Available online 31 May 2005

Abstract

Experiments reveal that the lattice constants of nanocrystallites with the number of CeO_{2-x} formula units N more than 68 expand relative to the bulk CeO_2 but are very different depending on the fabrication method. Densities of states are calculated for bulk CeO_2 and $CeO_{1.5}$, and for $(CeO_2)_{13}$ and $(CeO_{1.5})_{13}$ clusters. Band gap energies of the bulk CeO_2 and $CeO_{1.5}$ are estimated to be 3.20 and 0.30 eV, respectively. HOMO–LUMO gap energies of the clusters $(CeO_2)_{13}$ and $(CeO_{1.5})_{13}$ are calculated to be almost 0 and 3.05 eV, respectively. Experimental results of the ultraviolet absorption of nanocrystallites with the number of CeO_2 and $CeO_{1.5}$ formula units more than 68 show the blueshifts from the bulk CeO_2 and $CeO_{1.5}$, respectively, due to the quantum confinement effect.

Keywords: Cerium oxide; Nanocrystallite; Cluster; Core–shell structure; Band gap energy; Ab initio calculation; Size effect

1. Introduction

Cerium oxides have attracted intensive attention as ultraviolet (UV) absorbents [1] and for catalytic redox reactions in order to clean the exhaust of automobiles [2]. The catalytic effect comes from the reversible chemical reaction between the two cerium oxides, the oxygen-rich CeO_2 and the oxygen-poor Ce_2O_3, depending on the chemical potential of oxygen. For this reason, some studies on the electronic, bonding and optical properties of cerium oxide bulk crystals have been carried out from both fundamental and technological viewpoints [3]. Recently, blueshifts in UV absorption spectra of monodisperse cerium oxide nanocrystallites have been found for the direct optical transition [4]. It is very useful to be able to control the position of the UV absorption edge by particle sizes. Very recently, X-ray diffraction studies have shown that the synthesized cerium oxide nanocrystallites have a cubic fluorite-type structure and large lattice expansions [5]. This is in contrast to a decrease often observed in the lattice constant of metal nanoparticles with decreasing particle size. The core level shift of Ce 3d in X-ray photoelectron spectra of cerium oxide (CeO_{2-x}; $0 \leqq x \leqq 0.5$) nanocrystallites has revealed that the effective valence state of Ce ions is 3.0 for a diameter of about 1.4 ± 0.2 nm [6], which corresponds to $CeO_{1.5}$-type cluster with $N = 68$. It has been shown that the change in the lattice constant is in good correlation with the change in the valence state for cerium oxide nanocrystallites [5,6]. On the other hand, the structures of $(CeO_2)_N$ and $(CeO_{1.5})_N$ clusters were previously determined by simulated annealing with classical interatomic potentials and showed that the former is reduced in size independent of the values of N and the latter is extended with decreasing cluster size down to $N = 13$ [7]. The size effect of such a material in the range of nanometers is very interesting but has not been well researched.

In this report, the effects of the lattice constants (or bondlengths) and electron gap energies on the particle sizes in the range from nano- to subnano-meters are clarified by both the experiments and computations.

* Corresponding author. Fax: +81 22 215 2101.
E-mail address: scorpion@imr.edu (S. Tsunekawa).

0925-8388/$ – see front matter © 2005 Elsevier B.V. All rights reserved.
doi:10.1016/j.jallcom.2004.12.140

2. Experiments and calculations

Measurements of lattice constants were carried out for monosized cerium oxide nanocrystalline particles S1, S2 and S3 having diameters of 8.6 ± 1.3, 3.8 ± 0.6 and 2.2 ± 0.3 nm, respectively, prepared by the successive microemulsification method [8] using X-ray powder diffractometer (Geigerflex, Rigaku) in the 2θ range 20–70° with a Cu Kα irradiation, where the size range indicates the standard deviation of the particle diameter.

Measurements of absorbance (optical density, OD) spectra were performed for monodisperse cerium oxide toluene sols with a series of diameters 2.2 ± 0.3, 2.7 ± 0.4 and 3.2 ± 0.5 nm in 10 mm quartz cuvettes using a UV–VIS spectrophotometer (U-2000, Hitachi) with a deuterium lamp, where $\mathrm{OD} \equiv \log(I_0/I)$, where I_0 and I are the intensities before and after transition. The examination for the OD data was performed with a conventional method for direct optical transition [4].

The band structure and/or the densities of states (DOS) were calculated for CeO_2 and $CeO_{1.5}$ bulk crystals, and $(CeO_2)_{13}$ and $(CeO_{1.5})_{13}$ clusters using the self-consistent full potential linearized augmented-plane-wave method under the generalized gradient approximation with spin–orbit coupling [9]. The lattice constants were set to the experimental values (0.5411 nm for CeO_2 and 1.122 nm for $CeO_{1.5}$).

3. Results and discussion

The size dependence of the lattice constants for the present samples S1, S2 and S3 is shown in Fig. 1. $\log(\Delta a)$–$\log(D)$ plot is represented in the inset, where $\Delta a = a - a_0$; a_0 is the lattice constant of the bulk CeO_2 and D is the particle diameter. The relation is obtained from the figure:

$$\Delta a = 0.0324 D^{-0.98} \quad \text{(nm)}. \tag{1}$$

Recently, another size dependence of the lattice constants has been reported by Wu et al. [10] (see Fig. 1 and the inset):

$$\Delta a = 0.0600 D^{-1.05} \quad \text{(nm)}. \tag{2}$$

This relation was obtained by applying the $\log(\Delta a)$–$\log(D)$ plot to their size dependence curve. Their nanoparticles (about 3–20 nm in diameter) were made in Helium atmosphere (about 1–100 Torr) at about 2000 °C by a vapor phase condensation method. The outlines of the particles were mostly circular or ellipsoidal, quite different from the nanoparticles with octahedral shape and surrounded by {1 1 1} planes previously reported by Zhang et al. [11] who made the monosized nanoparticles by mixing cerium nitrate solution with an ammonium reagent and the heat treatment at 400–800 °C for 30 min (about 6–80 nm in diameter). Fig. 1 also shows the different types of the size dependence of the lattice constants obtained by Zhang et al. [11]. From this figure, it is suggested that while the lattice constants of the particles with octahedral shape are little dependent on size, those with circular or ellipsoidal shape strongly depend on size. Conesa has proposed the order of surface stabilization of unionized isolated oxygen vacancy defects in the bulk CeO_2 by computer simulations [12]: (1 1 1) < (1 0 0) < (1 1 0) < (2 1 1) < (2 1 0) < (3 1 0). Therefore, the above size dependences should be explained by the surface stability due to oxygen vacancies. It is reasonable that the present size dependence is located at the middle position, because the present samples partially dissolve in strong acid [8] and include both the polyhedral and round shaped particles as shown in Fig. 2. This is explained by the Berg effect [13], which acts preferentially on the edges of polyhedral crystallites with larger sizes on both dissolution

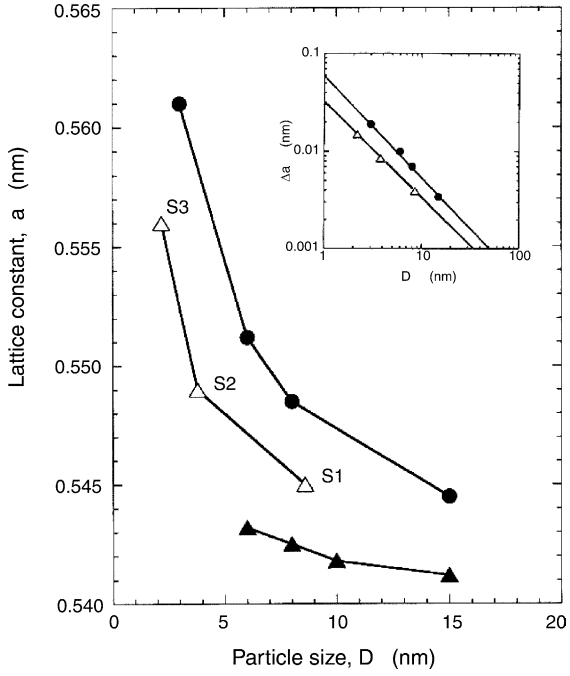

Fig. 1. Lattice constants as a function of the particle diameter: Wu et al. (●); Tsunekawa et al. (the present result) (△); Zhang et al. (▲). The inset represents the $\log(a)$–$\log(D)$ plots for the results of Wu et al. (●) and Tsunekawa et al. (△).

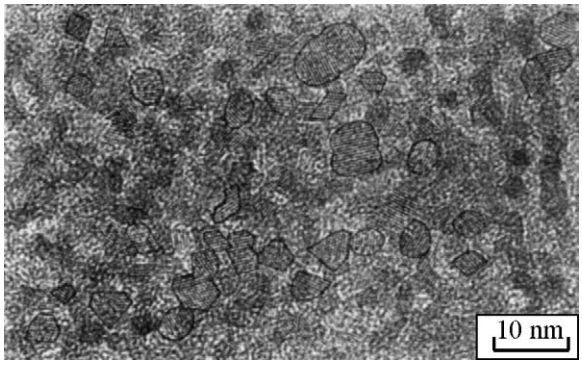

Fig. 2. Typical high-resolution transmission electron microscopic image of the present nanoparticles. Only the outlines of the particles with clear {1 1 1} lattice fringe images are illustrated by the solid line.

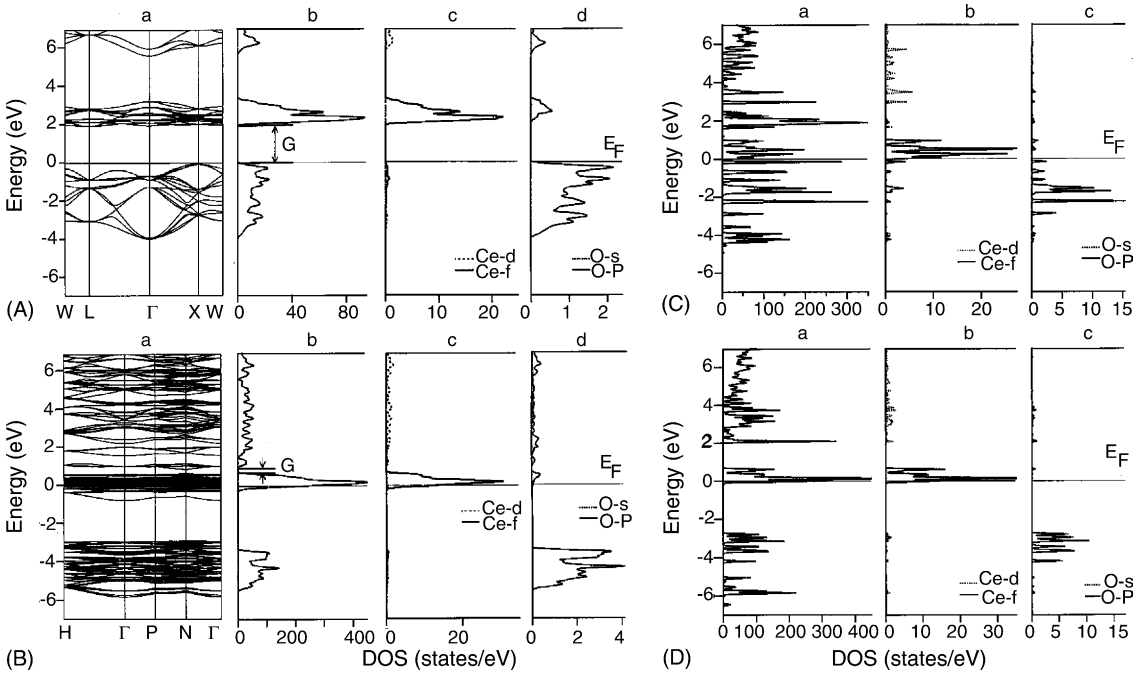

Fig. 3. Band calculations for CeO_2 (A) and $CeO_{1.5}$ (B) bulk crystals: band structure (a), total DOS (b), and partial DOS of Ce (c) and O (d). Computed DOS for $(CeO_2)_{13}$ (C) and $(CeO_{1.5})_{13}$ (D) clusters: total DOS (a), and partial DOS of Ce (b) and O (c). The thin lines denote the Fermi energy, E_F, levels. "*G*" indicates the band gap.

and growth. The above results strongly suggest that the octahedral cerium oxide nanocrystallites with {1 1 1} planes are a poor catalyst for oxidation.

Wu et al. have clarified by electron energy-loss spectroscopy that Ce^{3+} ions in relatively large CeO_{2-x} nanoparticles are primarily in the surface regions and are unevenly dispersed throughout a particle [10]. This is reasonable because the Ce^{4+} and Ce^{3+} ions coexist in the X-ray photoelectron spectra as previously reported [6]. We call this "core–shell structure" for the CeO_{2-x} nanoparticles. Using this model (the Ce_2O_3 shell and the CeO_2 core), we can estimate the thickness of $CeO_{1.5}$ surface layer, t, in our nanoparticles: $0.28\,\text{nm} \leqq t \leqq 0.56\,\text{nm}$ [14]. This reveals that the thickness of the Ce_2O_3 shell is at most 0.561 nm, which well explain the size dependence of the lattice constant in our samples. We can also determine the thickness of the surface layer, t', for Wu et al.'s samples [Eq. (2)] to be $0.421\,\text{nm} \leqq t' \leqq 0.561\,\text{nm}$.

Fig. 3(A and B) shows the computed band structures and the DOS of the bulk CeO_2 and $CeO_{1.5}$. The band gap energies in CeO_2 and $CeO_{1.5}$ are 3.20 and 0.3 eV, respectively, where the band gap energies are multiplied by a factor of 1.7 in order to match the experimental value of bulk CeO_2. It should be noted that the optical transitions for CeO_2 and $CeO_{1.5}$ occur directly at the Brillouin zones, X (1, 0, 0) and N (0, 0, 0.5), respectively, from the band structures, but the types are different, i.e., charge-transfer transition from O 2p-like band to Ce 4f-like band for CeO_2 and electronic transition from Ce 4f-like band to Ce 5d-like band for $CeO_{1.5}$. Experiments reveal the blueshifts in both the optical transitions with the decrease in size as shown in Fig. 4 and the

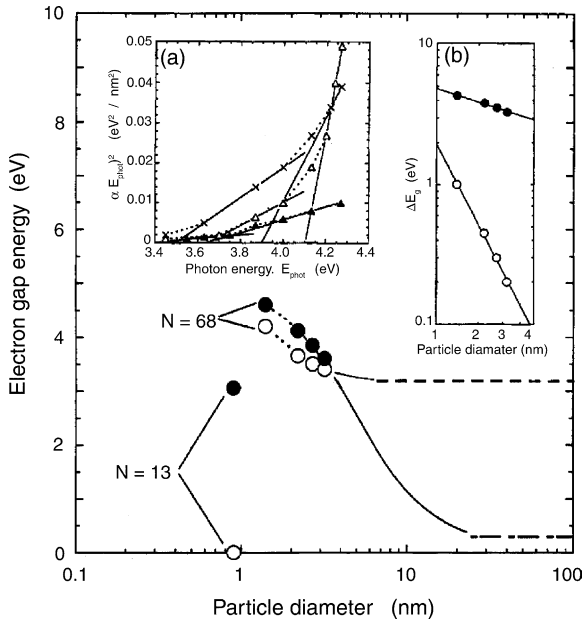

Fig. 4. Size dependence of the band gap energies for CeO_2 (◯) and $CeO_{1.5}$ (●) nanocrystallites and the HOMO–LUMO gap energies for $(CeO_2)_{13}$ (◯) and $(CeO_{1.5})_{13}$ (●) clusters. The dashed line indicates the band gap energy of bulk CeO_2 and the dashed–dotted line represents that of bulk $CeO_{1.5}$. The insets show the plot of $(\alpha E_{phot})^2$ vs. photon energy for the particles of 2.2 nm (△), 2.7 nm (×) and 3.2 nm (▲) in diameter (a) and the plot of ΔE_g vs. particle diameter in cerium oxide nanocrystallites (b), where $\alpha = \text{OD}/d$ (OD is optical density); $d = (lC/\rho)$ (l is the light path length, C the concentration of the toluene sols and ρ is the density of the bulk); $E_{phot} = 1240/\lambda$ (eV) (λ is the light wavelength in the unit of nanometer); $\Delta E_g = E_g - 3.20$ (eV) for CeO_2 (◯) and $\Delta E_g = E_g - 0.30$ (eV) for $CeO_{1.5}$ (●), and the band gap energy E_g is obtained from the photon energy extrapolated to $\alpha = 0$.

insets (a and b): $E_g = 3.20 + 2.31D^{-2.15}$ (eV) for CeO_2 and $E_g = 0.30 + 5.15D^{-0.39}$ (eV) for $CeO_{1.5}$ in the nanosize range up to 5 nm diameter. This is considered to be a quantum confinement effect [15] well known in nanosize materials. Fig. 3(C and D) shows the computed DOS of $(CeO_2)_{13}$ and $(CeO_{1.5})_{13}$ clusters which have the minimum size with a cubic fluorite-type structure. The HOMO–LUMO gap energies multiplied by the same factor 1.7 are also indicated in Fig. 4. It is revealed that the gap energies of the clusters $(CeO_2)_{13}$ and $(CeO_{1.5})_{13}$, ~0 and 3.06 eV, respectively, are much lowered from those of the clusters $(CeO_2)_{68}$ and $(CeO_{1.5})_{68}$ corresponding to nanocrystalline particles with the diameter of about 1.2 nm, 4.20 and 4.60 eV, respectively, estimated from the above-mentioned blueshift. This is expected to be due to the cluster effect [16] between nano- and subnano-meter sizes.

Acknowledgments

We are grateful to the staff of the Center for Computational Materials Science at IMR (Tohoku University) for their continuous support of the supercomputer facilities. J.-T. Wang would like to thank the JSPS for the financial support.

References

[1] S. Yabe, S. Momose, J. Soc. Cosmet. Chem. Jpn. 32 (1998) 372.
[2] J.Y. Ying, A. Tschöpe, Chem. Eng. J. 64 (1996) 225.
[3] N.V. Skorodumova, R. Ahuja, S.I. Simak, I.A. Abrikosov, B. Johansson, B.I. Lundqvist, Phys. Rev. B 64 (2001) 115108.
[4] S. Tsunekawa, T. Fukuda, A. Kasuya, J. Appl. Phys. 87 (2000) 1318.
[5] S. Tsunekawa, R. Sahara, Y. Kawazoe, K. Ishikawa, Appl. Surf. Sci. 152 (1999) 53.
[6] S. Tsunekawa, T. Fukuda, A. Kasuya, Surf. Sci. 457 (2000) L437.
[7] S. Tsunekawa, J.-T. Wang, Y. Kawazoe, Abstract of Symposium on Rare Earths, Rare Earth Society of Japan, Osaka, 2002, p. 48.
[8] S. Tsunekawa, R. Sivamohan, T. Ohsuna, A. Kasuya, H. Takahashi, K. Tohji, Mater. Sci. Forum 315–317 (1999) 439.
[9] G. Kresse, J. Hafner, Phys. Rev. B 48 (1993) 13115;
G. Kresse, J. Furthmüller, J. Comput. Mater. Sci. 6 (1996) 15.
[10] L. Wu, H.J. Wiesmann, A.R. Moodenbaugh, R.F. Klie, Y. Zhu, D.O. Welch, M. Suenaga, Phys. Rev. B 69 (2004) 125415.
[11] F. Zhang, S.-W. Chan, J.E. Spanier, E. Apak, Q. Jin, R.D. Robinson, I.P. Hermann, Appl. Phys. Lett. 80 (2002) 127.
[12] J.C. Conesa, Surf. Sci. 339 (1995) 337.
[13] C.W. Bunn, Discuss. Faraday Soc. 5 (1949) 132.
[14] S. Tsunekawa, S. Ito, Y. Kawazoe, Appl. Phys. Lett. 85 (2004) 3845.
[15] I. Kosacki, V. Petrovsky, H.U. Anderson, Appl. Phys. Lett. 74 (1999) 34.
[16] V. Kumar, Y. Kawazoe, Phys. Rev. B 66 (2002) 144413.